Progress In Electromagnetics Research C, Vol. 23, 191–203, 2011

DESIGN OF NOVEL CPW CROSS-FED ANTENNA

S. Lin [1, 2, *], G.-L. Huang [2], R.-N. Cai [2], X. Y. Zhang [2], and X. Q. Zhang [2]

[1]Electronic Science and Technology Post-doctoral Research Center, Harbin Institute of Technology, Harbin 150080, China

[2]School of Electronics and Information Engineering, Harbin Institute of Technology, Harbin 150080, China

Abstract—A novel coplannar waveguide (CPW) cross-fed antenna which is wideband, high-gain and omnidirectional is proposed. After simulating the antenna model by CST MICROWAVE STUDIO®, the results show that this antenna not only has compact size, but also can effectively broaden operating band, improve gain and remain omnidirectional. In addition, adjusting antenna elements' dimension and spacing can control the central frequency position of operating band and bandwidth. The simulated results of antenna surface currents can be used to explain the reason of antenna possessing broadband and omnidirectional high-gain characteristics. A CPW cross-fed antenna operating at 2.4 GHz is designed and manufactured for measurement. The prototype is printed on a FR-4 epoxy resin board with 1 mm thickness. The experimental results indicate that the operating band is 2.35–2.85 GHz with reflection coefficient less than −10 dB (relative bandwidth 19.2%), and maximum gain in H-plane can achieve 5.2 dBi. Measured results well match the simulated ones. Moreover, the total antenna size is 187 mm × 22.5 mm ($1.5\lambda \times 0.18\lambda$), which can make it suitable in WLAN systems.

1. INTRODUCTION

In the field of wireless communication, omnidirectional antennas are widely applied into one-point-to-multipoint communication, broadcasting, data transmission and other fields. The emergence of printed antenna has provided some new fabrication ways for antenna

Received 1 July 2011, Accepted 3 August 2011, Scheduled 16 August 2011

* Corresponding author: Shu Lin (linshu@hit.edu.cn).

miniaturization and batch production. In recent years, researchers have also proposed some new omnidirectional antenna structures. Rmili et al. proposed a dual-band printed dipole antenna for IMT-2000 and 5 GHz WLAN (Wireless Local Area Network) application [1]. Kung et al. also proposed a similar model as Rmili's and printed balum on the substrate for coupling feeding, but this antenna does not have high gain [2]. Hwang et al. had manufactured a coaxial-fed antenna working in ISM-band and its impedance bandwidth is 400 MHz with reflection coefficient less than −10 dB, and the maximum gain is 1.4 dBi in the band [3]. Liu and Su proposed a square cylindrical monopole antenna fabricated using a cross-shaped metal plate. Although it is wideband, it can not achieve high-gain in low-frequency band [4]. Wong et al. designed a high-gain and omnidirectional CTS antenna, but it is difficult for prototype tuning and not suitable for batch production [5].

As the representative of early omnidirectional antenna, coaxial collinear (COCO) antenna has been widely applied to engineering practice shortly after Balsley and Ecklund first proposed it [6]. Then researchers have theoretically analyzed the working principle about COCO antenna and proposed some equivalent circuit models [7]. Based on the cylindrical antenna equation, Judasz et al. have analyzed the current distribution of COCO antenna, impedance characteristic and radiation model [8]. Litva et al. have established the integral equation of transmission line equivalent modeling, which is suited for COCO antenna analysis, and then used CG-FFT (Conjugate Gradient with Fast Fourier Transform) and FDTD (Finite Difference Time Domain) algorithms to solve the integral equation [9]. From the theoretical analysis, the current and phase of each COCO antenna's element should be equivalent respectively in order to achieve omnidirectional high-gain. Considering COCO antenna as a sequential-fed array, increasing the number of elements can easily improve antenna gain. However, the harmonic structure of this antenna makes the bandwidth become a key factor for antenna performance, e.g., a high gain COCO antenna is presented in [10], but its relative bandwidth is narrow. In order to achieve broadband, Zhou et al. proposed a method of rotating COCO antenna's elements, namely, an element rotated a certain angle different from its two adjacent elements [11]. In addition, increasing elements' spacing or adding a sleeve on the top of COCO antenna can also broaden the antenna operating bandwidth, but in this case, antenna gain is unsatisfying, as well as enlarging antenna size. Moreover, the manufacture of this antenna is not easy to achieve consistency, and it can be only used in HF or VHF band.

In recent years, the development of wideband printed dipole antenna (WPDA) provides some new optional methods to solve the problems above. Gao et al. proposed an improved printed dipole array antenna based on a perpendicular polarization omnidirectional antenna [12]. Its relative bandwidth is 5.7% with VSWR < 1.5, out-of-roundness of the radiation pattern is less than 0.6 dB and the maximum gain is 7.8 dBi in operating band.

In this paper, combined with printed antenna technologies and printed WLAN antenna models [13], a novel printed CPW cross-fed antenna with metal via-holes is proposed. The characteristics of broadband, high-gain and omnidirectional antenna can be obtained, and the operating bandwidth can cover the WLAN band from 2.412 GHz to 2.482 GHz (IEEE 802.11.b and IEEE 802.11.g) and ISM (Industrial Scientific and Medical) band. A terminal matcher has been designed to ensure the antenna can achieve wideband. What's more, several via-hole connectors are introduced into the CPW feeding, which can make the proposed antenna possess omnidirectional high-gain in H-plane. The parameters of antenna structure are optimized by CST MWS®, and the simulated results of surface currents can be used to explain the reason that the antenna can achieve broadband and omnidirectional high-gain. Finally, the antenna's prototype is manufactured and measured in anechoic chamber to ensure the feasibility of design idea. The proposed antenna has simple-structure, which is easy for manufacture and has a promising application future.

2. ANTENNA DESIGN

2.1. Antenna Structure

The structure of CPW cross-fed printed antenna is shown in Fig. 1. The antenna is printed on double-side of a FR-4 epoxy resin board with permittivity $\varepsilon_r = 4.5$ and thickness $h = 1$ mm. The position relationship of printed metal on the front side and back side is also presented in Fig. 1. Then the total antenna structure can be divided into three parts, including CPW cross-fed part, terminal matching part and the via-hole connectors on the back side. Four CPW feeding-line elements are arranged from top to bottom in the front side, and a triangle metal patch is connected with the central feeding-line in the top terminal. In the back side, there are four metal connectors linking the grounds through via-holes in both sides of CPW central feeding-line. The values of structural parameters are: $d = 17$ mm, $g = 1.5$ mm, $h = 1$ mm, $l_1 = l_6 = 30$ mm, $l_2 = l_4 = 28$ mm, $l_3 = 15$ mm, $r = 0.25$ mm, $w_1 = 2$ mm and $w_2 = 7$ mm.

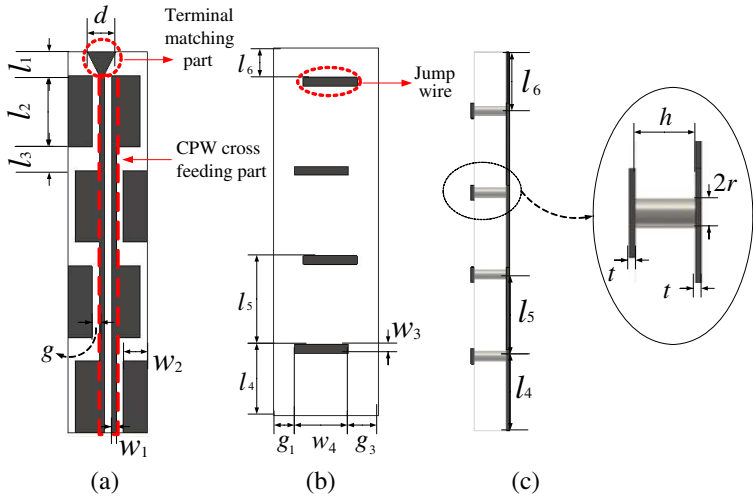

Figure 1. Sketch of the proposed antenna with associated geometrical parameters. (a) Front view. (b) Back view. (c) Transverse view.

2.2. Antenna Working Principle

The proposed antenna has some similarities with the COCO antenna presented in [6], but the main difference is that it is transformed from spatial structure to planar structure, shown in Fig. 2. When the excitation current feeds the feeding-line from the bottom, the current would flow along the cross-connected transmission line, and the current distribution would be established on the transmission line. When the current flows to the terminal triangle patch, the current distribution would be also established on it. Because the triangle patch, CPW metal-line and the ground can form a triangle monopole antenna and its own current can radiate to the free-space, so the total antenna terminal is equal to be connected with a matching load. During the operating bandwidth of the triangle monopole antenna, the currents on the CPW cross feeding-line are traveling-wave current. This is the crucial difference between the opening CPW cross-feed antenna and traditional COCO antenna. All the currents on COCO antenna are standing-wave current. So this difference can make the bandwidth of CPW cross-feed antenna wider than traditional COCO antenna. The traveling-wave current would also excite the current distribution on the other CPW ground through the via-hole connectors. But the currents of this part are standing-wave current and the resonant frequency would be constricted by the ground size l, which can be calculated by formula (1), where ε_e is the effective permittivity after considering

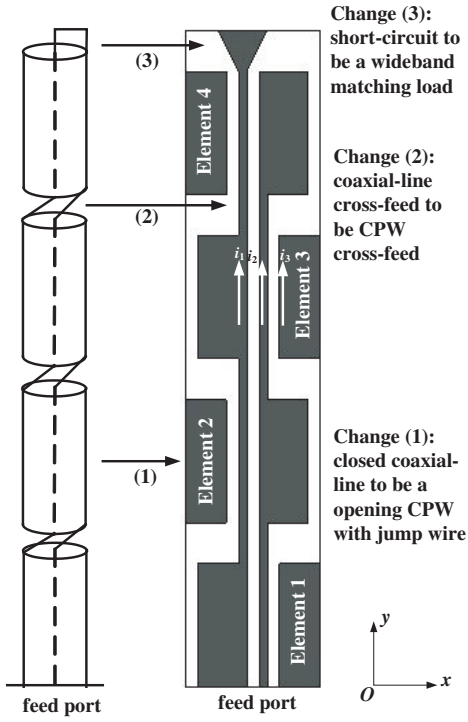

Figure 2. The transformation of antenna structure.

the substrate's influence.

$$f = \frac{c}{2l\sqrt{\varepsilon_e}} \tag{1}$$

Regards to one of antenna's elements, after the simulation by CST software, we can obtain currents of the three parts, which flow along the $+y$ direction, indicated by i_1, i_2 and i_3. The current amplitudes of the three parts are so large that they play a crucial role in antenna radiation. As shown in Fig. 2, i_1 and i_2 are equi-amplitude and reverse-phase, so the radiations of the two parts' currents counteract with each other, and then the radiation of i_3 decides antenna radiation patterns and other characteristics. Based on the discussion above, if we want to improve antenna gain, the feeding spacing is required to be adjusted to control the phases of i_3, which can make the phases achieve in-phase stacking in farfield. Since the length of element (l) decides i_3's resonant frequency, the antenna operating frequency can be adjusted through changing l.

3. SIMULATION AND ANALYSIS

According to the analysis and discussion of antenna working principle above, the characteristics of impedance and radiation can be explained by the simulated results of antenna surface currents. Fig. 3 shows the current distribution curve of transmission line in CPW cross-feed part. At the typical frequency 2.5 GHz, the current is traveling-standing-wave current, and the normalized amplitude is 0.44. VSWR at this frequency can be calculated out 2.27 and the reflection coefficient is −8.2 dB. The calculated result is the same as the simulated reflection coefficient (−10 dB@2.5 GHz).

The traveling-standing-wave currents are fed into CPW uncross-fed ground, which can create standing-wave current (as shown in Fig. 4, @2.5 GHz) and determine antenna radiation characteristics. The edge-current's amplitude distribution of uncross-fed grounds of the four

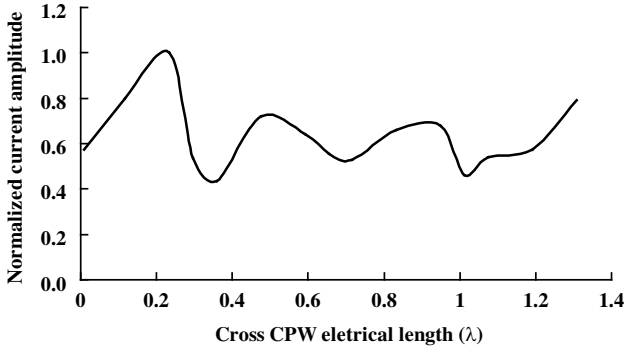

Figure 3. The current of transmission line in CPW cross-feed part.

Table 1. Normalized current distribution of four radiation elements at typical frequency.

Frequency	2.3 GHz	2.5 GHz	2.7 GHz
Equivalent amplitude and phase of Element1	$0.60 \angle -47.7°$	$0.93 \angle -60.1°$	$0.70 \angle -60.0°$
Equivalent amplitude and phase of Element2	$0.88 \angle -0.1°$	$1.00 \angle -64.4°$	$0.60 \angle -98.5°$
Equivalent amplitude and phase of Element3	$0.88 \angle -0.1°$	$0.93 \angle -59.9°$	$1.00 \angle -125.4°$
Equivalent amplitude and phase of Element4	$1.00 \angle 8.8°$	$1.00 \angle -76.4°$	$0.96 \angle -146.9°$

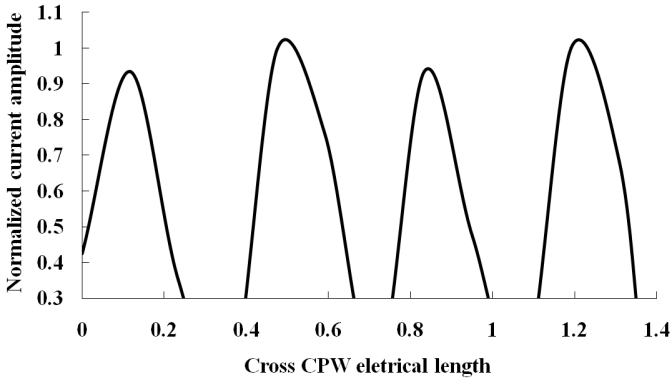

Figure 4. Normalized current distribution of four radiation elements.

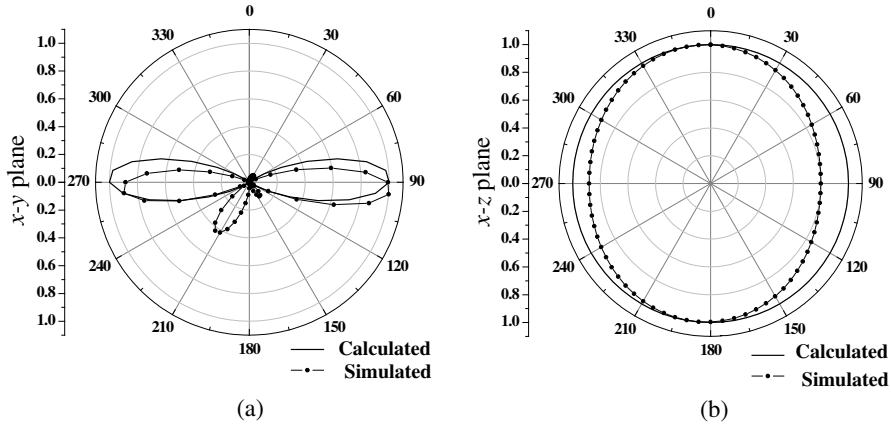

Figure 5. Antenna normalized power pattern. (a) E-plane. (b) H-plane.

antenna elements is presented in Table 1, and it can be seen from the table that there is little difference between the amplitude of the four elements' current-amplitude at 2.3 GHz, 2.5 GHz and 2.7 GHz, respectively. What's more, the phases are nearly the same in a wide bandwidth or phase-difference less than $\pi/2$, which indicate that, in this bandwidth, the radiation mode of the proposed antenna is equivalent to the side-fire array and it can form omnidirectional radiation. Its directivity functions can be described by formulas (2)–(4), where δ — the angle between viewing direction and antenna axis; m_i — the ratio of Element i's and Element l's standing-wave

current amplitudes. It should be emphasized that in Table 1, the current amplitudes are the normalized amplitudes; φ_i — the phase of the Element i's standing-wave current; k — the wave number, $k = 2\pi/\lambda$; d — the distance between elements' center, in this paper, $d = l_2 + l_3 = 43\,\text{mm}$. Due to the poor current distribution on terminal load, its radiation can be omitted in the influence of antenna pattern. In formula (2), the dipole element can be equivalent to a half-wave dipole and the array-element function can take $\cos[(\pi/2)\sin\delta]/\cos\delta$. The reason is that, as the simulated results shown in Fig. 4, the currents distribute on the antenna elements, whose length is 3/10 of wavelength of free space. But the currents of elements' upper and lower ends are not zero, and the current distribution is similar to cosine distribution, as the half-wave dipole. The following calculated results indicate that the error of the above analysis method is small.

$$f_E(\delta) = \frac{\cos\left(\frac{\pi}{2}\sin\delta\right)}{\cos\delta} \cdot \left[\left(\sum_{i=1}^{4} \frac{m_i}{m_1}\cos\psi_i\right)^2 + \left(\sum_{i=1}^{4} \frac{m_i}{m_1}\sin\psi_i\right)^2\right]^{\frac{1}{2}} \quad (2)$$

$$f_H(\delta) = \left[\left(\sum_{i=1}^{4} \frac{m_i}{m_1}\cos\psi_i\right)^2 + \left(\sum_{i=1}^{4} \frac{m_i}{m_1}\sin\psi_i\right)^2\right]^{\frac{1}{2}} \quad (3)$$

$$\psi_i = \varphi_i - \varphi_1 + (i-1)kd\cos\delta, \quad i = 1,\, 2,\, 3,\, 4 \quad (4)$$

According to formulas (2)–(4), the antenna normalized power patterns (@2.5 GHz) can be drawn out. The calculated results are: $m_1 = 1.0$, $\varphi_1 = -60.1^\circ = -1.05\,\text{rad}$, $m_2 = 1.065$, $\varphi_2 = -64.4^\circ = -1.12\,\text{rad}$, $m_3 = 1.0^\circ$, $\varphi_3 = -59.9^\circ = -1.05\,\text{rad}$, $m_4 = 1.07^\circ$ and $\varphi_4 = -76.4^\circ = -1.33\,\text{rad}$. All these current amplitudes are compared with the current amplitude I_1 of Element 1. The comparison between the calculated patterns and simulated results are presented in Fig. 5. The two well match with each other in the tendency, except the lobe width and out-of-roundness. Because the substrate and non-axisymmetric structure would influence the simulated results, the out-of-roundness would be in radiation patterns. In addition, the calculated model is a co-axial linear antenna model, which is an absolutely axisymmetric model, so the difference exists between the calculated and simulated models, but this difference can be accepted. After calculating, the maximum level error is 1 dB, which indicates that using the equivalent radiation model of current phase array can describe the antenna radiation characteristic.

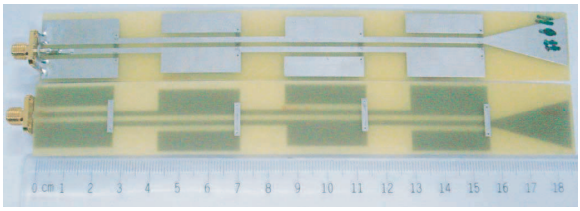

Figure 6. Antenna prototype.

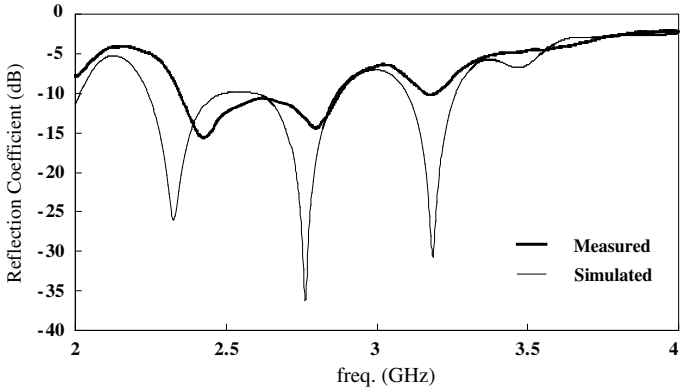

Figure 7. The simulated and measured results of reflection coefficient.

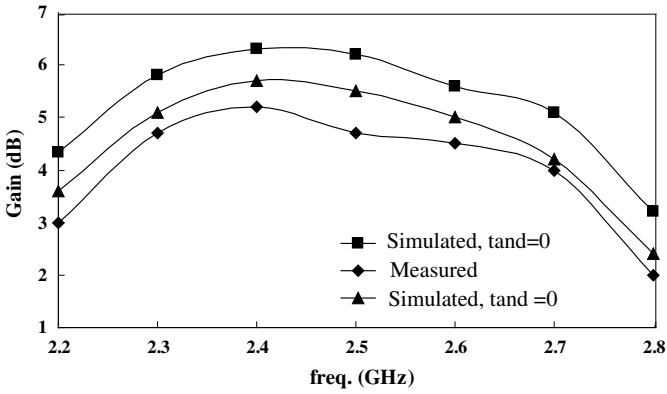

Figure 8. The simulated and measured results of antenna gain.

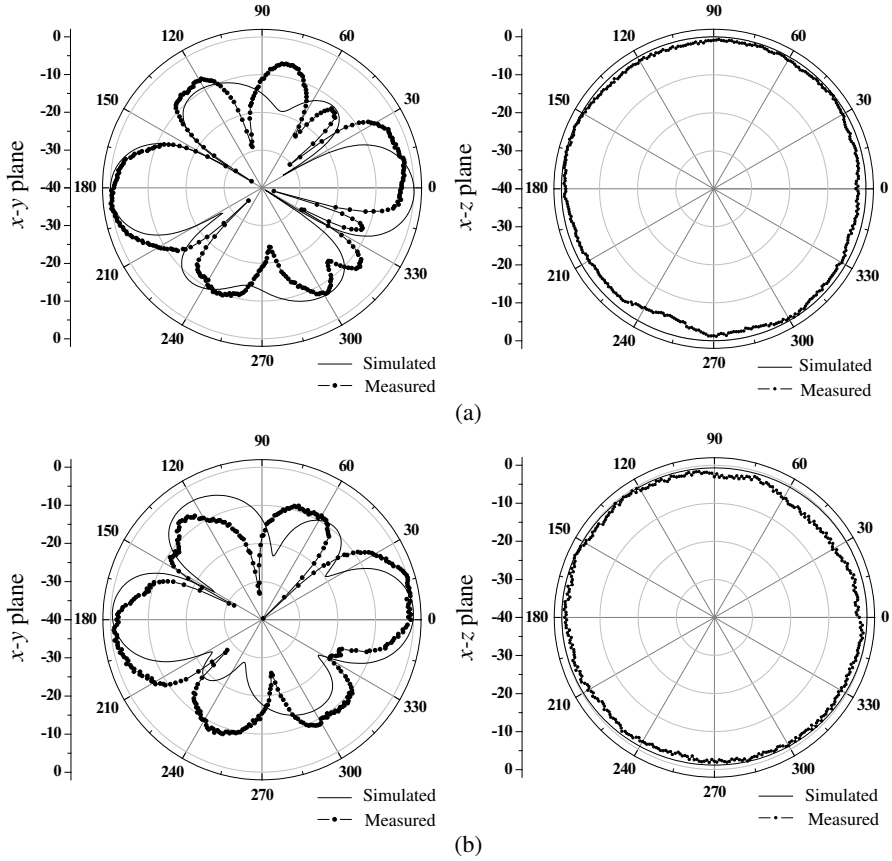

Figure 9. The normalized radiation pattern for 2.4 GHz and 2.5 GHz. (a) The simulated and measured results of radiation patterns at 2.4 GHz: E-plane (Left), H-plane (Right). (b) The simulated and measured results of radiation patterns at 2.5 GHz: E-plane (Left), H-plane (Right).

4. EXPERIMENTAL RESULTS AND ANALYSIS

According to the simulated results, an antenna prototype (Figure 6) has been manufactured and measured in anechoic chamber, using the Agilent E8363B Vector Network Analyzer and the experimental results are shown in Figs. 7–9. From Fig. 7, the operating bandwidth of the proposed antenna is 2.35–2.85 GHz with reflection coefficient less than -10 dB (relative bandwidth 19.2%), which is a little smaller than the simulated result (2.25–2.85 GHz), but both trends are consistent. The

reflection coefficient error is mainly caused by: (1) the reflection from feeding connector. This factor is not considered in the simulation. But the actual SMA connector is connected with CPW feeding port through manual welding, so the discreteness of welding would cause reflection in some frequency bands, which finally would cause reflection coefficient increase in the experimental results. (2) the substrate's inhomogeneity and discreteness. Both the inhomogeneity of substrate's relative permittivity and the discreteness from loss can cause the reflection, which can also make the reflection coefficient grow in the feeding port. Regards to the FR-4 epoxy resin board used in the prototype manufacture, its inhomogeneity and discreteness is strong so the reflection is also large.

The measured results of gain and radiation patterns are presented in Fig. 8 and Fig. 9. During the bandwidth 2.2–2.8 GHz, the measured maximum gain is about 1 dB lower than the simulated results. Actually, the perfect electrical conductor and perfect dielectric material are chosen as the antenna material of the simulated model, while the FR-4 epoxy resin board, using in the prototype manufacture, is lossy material with loss tangent 0.02. This is the main reason causing gain decrease. Therefore, we set the loss tangent of the substrate material to 0.02 ($\tan\delta = 0.02$) and re-simulated the antenna model. Fig. 8 shows that hte re-simulated result is close to the simulated. In addition, the measured results of radiation patterns well match the simulated except a small region (not exceed 10°), and the out-of-roundness of which is not satisfying, as shown in Fig. 9. It is probably caused by the inhomogeneity of relative permittivity. The omnidirectional gain is 5.0 dBi (maximum), and the gain difference would not exceed 3 dBi in the range of 2.2–2.8 GHz. All the results above indicate that the proposed antenna possesses broadband, high-gain and good omni-direction.

5. CONCLUSION

A novel CPW cross-fed printed antenna with broadband, high-gain and omnidirectional is proposed. Adjusting antenna elements' dimensions and spacing can control operating bandwidth and the position of central frequency. Then a prototype operating at WLAN band is manufactured, and the experimental results well match the simulated ones. The impedance bandwidth is 500 MHz (relative bandwidth 19.2%) with reflection coefficient less than −10 dB. The omnidirectional characteristic is fine in H-plane, and the out-of-roundness is less than 1.4 dB during the operating bandwidth. Antenna gain in the maximum radiation direction is better than 5.2 dBi. If

increasing the number of antenna elements, the gain would be further improved. Based on the simulation, an equivalent model of half-wave dipole array is pertinently proposed to explain the antenna working principle. The compact antenna is also easy for manufacturing and debugging. Therefore, the proposed antenna possesses a promising application future.

ACKNOWLEDGMENT

The authors would like to express their sincere gratitude to the funds supported by "the Fundamental Research Funds for the Central Universities" (Grant No. HIT.NSRIF.2010096) and the funds supported by "Heilongjiang post-doctorial financial assistance (LBH-Z09187)".

The authors would also like to thank CST Ltd. Germany, for providing the CST Training Center (Northeast China Region) at our university with a free package of CST MWS software.

REFERENCES

1. Rmili, H., J. M. Floc'h, P. Besnier, and M. Drissi, "A dual-band printed dipole antenna for IMT-2000 and 5-GHz WLAN applications," *Proceedings of the 9th European Conference on Wireless Technology*, Manchester, UK, Sep. 2006.
2. Kung, L., C. L. Yang, T. C. Tang, H. J. Chang, and W. B. Shie, "A dual-band printed dipole antenna with integrated balun covering UMTS and WiMAX bands," *Asia-Pacific Microwave Conference*, Asia Pacific, Dec. 2009.
3. Hwang, S. H., J. I. Moon, W. I. Kwak, and S. O. Park, "Printed compact dual band antenna for 2.4 and 5 GHz ISM band applications," *Electronics Letters*, Vol. 40, No. 25, Dec. 9, 2004.
4. Liu, Y.-T. and C.-W. Su, "Wideband omnidirectional operation monopole antenna," *Progress In Electromagnetics Research Letters*, Vol. 1, 255–261, 2008.
5. Wong, K.-L., F.-R. Hsiao, and T.-W. Chiou, "Omnidirectional planar dipole array antenna," *IEEE Transactions on Antennas and Propagation*, Vol. 52, No. 2, 624–628, 2004.
6. Balsley, B. B. and W. L. Ecklund, "A portable coaxial collinear antenna," *IEEE Trans. Antennas Propagat.*, Vol. 20, 513–516, 1972.
7. Mishustin, B. A., E. A. Redkina, and V. G. Slyozkin, "Coaxial collinear antennas with out-of-phase excitation of the elements,"

International Conference on Antenna Theory and Techniques, 504–506, Sevastopol, Ukraine, Sept. 9–12, 2003.

8. Judasz, T. J., W. L. Ecklund, and B. B. Balsley, "The coaxial collinear antenna: Current distribution from the cylindrical antenna equation," *IEEE Transactions on Antennas and Propagation*, Vol. 35, No. 3, Mar. 1987
9. Litva, J., Y. Zhuang, and A. Liang, "Modeling study of coaxial collinear antenna array," *Electrical and Computer Engineering*, Canadian Conference, Sept. 14–17, 1993.
10. Sakitani, A. and S. Egashira, "Analysis of coaxial collinear antenna: recurrence formula of voltage and admittance at connection," *IEEE AP*, Vo1. 39, No. 1, 15–20, Jan. 1990.
11. Zhou, Y.-Q., P. Lee, F. Jia, and B. Xu, "A technique for improving bandwidth of COCO antenna array," *4th International Conference on WiCOM.*, Oct. 12–14, 2008.
12. Gao, C. J., F. Guang, H.-Q. Zhang, and S.-D. Huo, "Design and research of an improved printed dipole array antenna," *Proceedings of 2009 National Annual Conference on Antenna*, Chengdu, China, Oct. 2009.
13. Li, X., L. Yang, S.-X. Gong, and Y.-J. Yang, "Bidirectional high gain antenna for WLAN application," *Progress In Electromagnetics Research Letters*, Vol. 6, 99–106, 2009.